J. Biochem. **135**, 139–148 (2004)
DOI: 10.1093/jb/mvh016

A Conserved Domain in the Tail Region of the *Saccharomyces cerevisiae* Na^+/H^+ Antiporter (Nha1p) Plays Important Roles in Localization and Salinity-Resistant Cell-Growth

Keiji Mitsui, Shinya Kamauchi, Norihiro Nakamura, Hiroki Inoue and Hiroshi Kanazawa*

Department of Biological Sciences, Graduate School of Science, Osaka University, 1-16 Machikaneyama-cho, Toyonaka City, Osaka 560-0043

Received October 24, 2003; accepted November 27, 2003

The *Saccharomyces cerevisiae* Na^+/H^+ antiporter Nha1p has a two-domain structure consisting of an N-terminal integral membrane region and a C-terminal cytoplasmic region. We previously identified six distinct cytoplasmic domains (C1–C6) conserved among yeast species and here we performed detailed structure-function analysis of the C1 domain (16 residues). Deletion of the C1 domain causes extensive inhibition of cell-growth under high salinity conditions. Mutants with single residue deletions or various amino acid substitutions affecting the C1 domain were analyzed with respect to salinity-dependent growth and Nha1p localization. The C1 domain was found to consist of two subdomains: (i) The first three N-proximal residues, which in conjunction with the integral membrane region play a crucial role in the targeting of Nha1p to the cytoplasmic membrane, and (ii) the portion between Leu-439 and Thr-449, which is not required for localization, but in which four residues (Gly-440, Arg-441, His-442, and Ile-446) affect salinity-sensitive cell-growth by possibly influencing the antiporter activity. Based on the overall similarity of the two-domain structure of Nha1p to that of mammalian Na^+/H^+ antiporters, the functional importance of domains proximal to the membrane region is discussed.

Key words: conserved domain, GFP fusion protein, hydrophilic tail, intracellular localization, site-directed mutagenesis, two-domain structure, Yeast Na^+/H^+ antiporter.

Cellular homeostasis requires that the pH and Na^+ concentration be maintained at certain levels in living cells (*1*, *2*). Na^+/H^+ antiporters play an important role in this regulation in organisms from bacteria to humans (*1*, *2*). Several Na^+/H^+ antiporters, also called Na^+/H^+ exchangers (NHEs), have been found in bacteria, yeast, plants and mammals (*3–7*). Although all antiporters are integral membrane proteins with the same function, their primary structures are diverse (*3–7*). Eight NHE isoforms have been reported for mammals (*8–12*) and their structure-function relationships have been extensively studied (*8–12*). As determined by hydropathy plot analysis, mammalian NHE isoforms have a two-domain structure consisting of an integral membrane region and a hydrophilic cytoplasmic tail region (*8–12*). The highly conserved integral membrane region is believed to form a structure essential for ion transport across the membrane (*8–12*). In contrast, the hydrophilic cytoplasmic region (tail region) is structurally diverse and accumulating evidence suggests that isoform-specific elements in this region mediate interactions with other proteins (*13–20*). However, the molecular details of these regulatory interactions remain to be determined.

Two Na^+/H^+ antiporters, Nhx1p and Nha1p, have been described in *Saccharomyces cerevisiae* (*21*, *22*). Nhx1p, which exhibits sequence homology with NHE6 (*10*, *23*, *24*), is a mitochondrial (*10*) and late-endosomal membrane protein (*23*, *24*) that drives Na^+ transport across membranes by means of a proton gradient that is probably formed by a V-type ATPase (*22*). Nha1p is transported to the cytoplasmic membranes from the endoplasmic reticulum (ER), and the Nha1p-mediated export of Na^+ is coupled to the proton motive force created by the plasma membrane H^+ translocating ATPase (*7*, *25*, *26*). Although sequences found in the integral membrane regions of mammalian NHE isoforms are not conserved in Nha1p, the yeast protein has a two-domain structure consisting of an integral membrane region and a hydrophilic membrane-peripheral region (the tail) (*27*), as found for mammalian NHEs. We have reported that six small but distinct conserved domains, C1 to C6, are present in the tail region, although the overall primary amino acid sequences of these domains vary among yeast species (*27*). We have also shown that these conserved domains likely have similar functions in yeast and other fungi (*27*). The C1 domain consists of sixteen residues, and the C2 (23 residues) and C3 (15 residues) domains, which are near the membrane region, are important for growth under conditions of high salinity, possibly by influencing the antiporter activity of Nha1p (*27*).

Here we further study the functions of the C1 domain, especially with respect to the intracellular localization of Nha1p. We demonstrate that C1 can be functionally dissected into two portions, one important for directing

*To whom correspondence should be addressed. E-mail: kanazawa@bio.sci.osaka-u.ac.jp

 © 2004 The Japanese Biochemical Society.

Downloaded from http://jb.oxfordjournals.org/ at Changhua Christian Hospital on September 29, 2012

intracellular localization and the other possibly required for ion transport. These findings provide new clues for understanding the functional significance of the two-domain structures of Nha1p and mammalian NHEs.

MATERIALS AND METHODS

E. coli and Yeast Strains, and Cell Culture—The *Saccharomyces cerevisiae* strains, G19 and SK5, used in this study are derivatives of W303–1B (MATα *leu2-3/112 ura3-1 trp1-1 his3-11/15 ade2-1 can1-100*) (*28*). G19 contains a deletion of *ENA1* (*ena1Δ::HIS3::ena4Δ*) (*28*) (a kind gift from Dr. A. Rodriguez-Navarro, Ciudad Univ.) and SK5 (*ena1Δ::HIS3::ena4Δ nha1Δ::LEU2*) (*27*) was derived from G19 by substitution of the 3.9 kb *Xba*I-*Nde*I *NHA1* fragment with *LEU2*. MTsec6, MTsec12, MTsec14, and MTsec18 are derived from YPH (MATa *ura3-52 lys2-80 ade2-10 trp1-Δ63 his3-Δ200 lue2-Δ1*) (kindly provided by Dr. Yoshinori Ohsumi, Naional Institute for Basic Biology and Dr. Akihiko Nakano, Univ. of Tokyo) (*29*) and bear the temperature sensitive alleles *sec6-4*, *sec12-4*, *sec14-3*, and *sec18-1*, respectively (*30*). In all experiments, cells were transformed with the vector alone or with one of the plasmids described below. Strains were routinely grown in rich medium (YPD) (*31*) containing 1% yeast extract, 2% peptone, and 2% glucose or minimal medium (SD) (*31*) containing 0.67% yeast nitrogen base and 2% glucose supplemented with required amino acids. *Escherichia coli* JM109 (*32*) was used for the propagation of plasmids. *E. coli* cells were cultured in L broth (*33*) at 37°C with an appropriate antibiotic for selection of transformants, as described previously (*33*). Solid media contained 1.5% agar.

Construction of Expression Vectors Encoding Nha1-GFP Fusions and Derivatives—Constructs encoding C-terminal truncations of Nha1p were created by amplification of the full *NHA1* open reading frame, and of the regions encoding amino acid residues 1–647 [NHA1Δ(C4-C6)], 1–449 [NHA1Δ(C2-C6)], and 1–433 [NHA1Δ(C1-C6)], with appropriate primers (Table 1) as described previously (*34*). All amplified DNAs were inserted between the unique *Kpn*I and *Sph*I restriction sites of pUC18, and the nucleotide sequences were verified. The full-length and truncation derivatives of Nha1p were tagged with the green fluorescent protein (GFP) as follows: A 0.7 kb GFP fragment was amplified from pEGFP-N3 (Clontech), and then cloned between the pUC18 *Sph*I and *Sal*I sites. *NHA1* and *NHA1* deletion derivatives were isolated from the above pUC18 derivatives by digestion with *Kpn*I and *Sph*I, and then ligated together with the *Sph*I–*Sal*I GFP fragment to *Kpn*I–*Sal*I–digested pKT10, a multi-copy yeast expression vector with the *GAP* promoter and terminator (*35*). The resulting plasmids, pP_{GAP}NHA1-GFP, pP_{GAP}NHA1Δ(C4-C6)-GFP, pP_{GAP}-NHA1Δ(C2-C6)-GFP, and pP_{GAP}-NHA1Δ(C1-C6)-GFP, were used to construct expression vectors carrying the *NHA1* promotor. The *Bam*HI fragment containing the 1.7 kb *GAP* promoter (one site lies within the pUC18 polylinker and the other within the *NHA1* coding sequence) was excised from these plasmids and replaced with a 1.6 kb genomic *Bam*HI fragment bearing the *NHA1* promoter. These plasmids were named pNHA1-GFP, pNHA1Δ(C4-C6)-GFP, pNHA1Δ(C2-C6)-GFP, and pNHA1Δ(C1-C6)-GFP. To create an internal deletion of the C1 domain in the full-length *NHA1*, oligos 6 and 7 (Table 1), which are specific to sequences flanking but not including the C1 domain, were used in conjunction with oligos 1 and 2 (Table 1) for PCR. The amplified fragment was used to replace the corresponding region of the *NHA1* expression vector pNHA1-GFP after digestion with *Bam*HI and *Sph*I. To create sequential deletions of the C1 domain, oligo 1 was used with oligos 8 to 18 (Table 1) to amplify a series of fragments encoding portions of Nha1p. The amplified sequences were used to replace the corresponding region of *Bam*HI–*Sph*I–digested pNHA1-GFP. Replacement of individual C1 residues by alanine or arginine, or replacement of three consecutive C1 residues by three consecutive alanine, serine or arginine residues was achieved by PCR with oligonucleotide primers carrying the desired mutations (Table 1, oligos 19 to 35 for single Ala replacement, 36 to 43 for triple Ala replacement, 44 to 45 for triple Ser or Arg replacement, and 46 to 48 for single Arg replacement with 1 and 2). Amplified DNA carrying replacements was substituted for the corresponding pNHA1-GFP sequence after digestion with appropriate restriction enzymes.

Growth Assays for Yeast Cells Transformed with Nha1-GFP Constructs—*NHA1*-deficient (SK5) and wild type (G19) cells transformed with the full-length *NHA1-GFP* fusion construct or derivatives were grown at 30°C for 24 h in SD, diluted and then grown for another 16 h in fresh medium. Exponential phase cells were then diluted 100-fold in SD, pH 5.5, and inoculated into 1 ml SD with various concentrations of NaCl in a multi-well plate. Growth was monitored spectrophotometrically (OD_{600}) and the relative growth rate was expressed as a percentage of the rate of growth in the absence of NaCl.

Detection of Cellular Localization of Nha1p-GFP by Fluorescence Microscopy—SK5 transformants expressing Nha1p-GFP fusion proteins or derivatives were inoculated at 30°C into SD, diluted and then incubated at 24°C in fresh medium. Early logarithmic phase cells were examined by fluorescence microscopy (Olympus BX51) with appropriate filter sets (NIBA).

sec mutants (*sec6-4, sec12-4, sec14-3,* and *sec18-1*) (*30*) transformed with the *NHA1-GFP* fusion construct were grown at 23°C in SD. The cultures were diluted with fresh medium, grown at 23°C to the early logarithmic phase, shifted to 37°C, and then incubated for another 2 h. Cells were fixed with cold methanol for 10 min at –20°C and then with cold acetone at –20°C. Cells were rehydrated with PBS and observed by fluorescence microscopy with appropriate filter sets.

Whole Cell Protein Fractionation and Western Blotting—Cells were grown to OD600 = 0.6–1.0, collected by centrifugation, resuspended in lysis buffer [20 mM Tris-HCl, pH 7.6, 0.2 M sorbitol, 5 mM EDTA, 10 mM PMSF, protease inhibitor cocktail (Roche Diagnostics)], and then disrupted with glass beads at 4°C. After removing unbroken cells and debris, a pellet fraction (P13) was obtained from the total lysate by centrifugation at 13,000 ×*g* for 15 min. The resulting supernatant was separated further into pellet (P100) and supernatant (S100) fractions by centrifugation at 100,000 ×*g* for 1 h (*39*). Each fraction was resuspended in an equal volume of SDS sample buffer. A 20 μg aliquot of each was subjected to SDS–polyacryla-

Downloaded from http://jb.oxfordjournals.org/ at Changhua Christian Hospital on September 29, 2012

Table 1. **Oligo DNAs used in this study.**

Oligo DNAs	Sequence (5′-3′)	Position*/Description
1. NHA1-*Bam*HI-Fw	TA$_{(i)}$GGATCCCTGCAGTCATGATA	1032–1053
2. SK31	TCT$_{(ii)}$GCATGCCCTTATTGAGACCA	2952–2964
3. SK29	TGT$_{(ii)}$GCATGCGGAGAGATGAAGAT	1938–1950 Δ(C4-C6)
4. SK32	TCT$_{(ii)}$GCATGCTGGTTAACGTTATC	1344–1357 Δ(C2-C6)
5. SK36	ATGA$_{(ii)}$GCATGCCTGAAGAACCATGAAC	1294–1308 Δ(C1-C6)
6. NHA1-ΔC1-Fw	CATGGTTCTTCAAAAACATTCACT	1294–1308, 1357–1368
7. NHA1-ΔC1-Rv	AGTGAATGTTTTTGAAGAACCATG	1294–1308, 1357–1368
8. NHA1-434-Rv	TCT$_{(ii)}$GCATGCTAACTGAAGAACCATG	1288–1302 NHA1–434
9. NHA1-435-Rv	TCT$_{(ii)}$GCATGCTTGCAACTGAAGAACC	1291–1305 NHA1–435
10. NHA1-436-Rv	TCT$_{(ii)}$GCATGCTGATTGCAACTGAAGAAC	1292–1308 NHA1–436
11. NHA1-437-Rv	TCT$_{(ii)}$GCATGCTTATGATTGCAACTGAAG	1295–1311 NHA1–437
12. NHA1-438-Rv	TCT$_{(ii)}$GCATGCTAGTTATGATTGCAAC	1300–1314 NHA1–438
13. NHA1-439-Rv	TCT$_{(ii)}$GCATGCTTAGAGTTATGATTGC	1303–1317 NHA1–439
14. NHA1-440-Rv	TCT$_{(ii)}$GCATGCTACCTAGAGTTATGATTG	1304–1320 NHA1–440
15. NHA1-441-Rv	TCT$_{(ii)}$GCATGCTACGACCTAGAGTTATG	1308–1323 NHA1–441
16. NHA1-442-Rv	TCT$_{(ii)}$GCATGCTATGACGACCTAGAGTT	1311–1326 NHA1–442
17. NHA1-443-Rv	TCT$_{(ii)}$GCATGCTCAAATGACGACCTAGAG	1313–1329 NHA1–443
18. NHA1-444-Rv	TCT$_{(ii)}$GCATGCTGTTCAAATGACGACCTAG	1315–1332 NHA1–444
19. V434A-Fw	GG$_{(iii)}$CTCGAGCGCTGCAATCATAACTCTAGG	1302–1328
20. I436A-Fw	GG$_{(iii)}$CTCGAGCGTTGCAGCCATAACTCTAGG	1302–1328
21. I437A-Fw	GG$_{(iii)}$CTCGAGCGTTGCAATCGCAACTCTAGG	1302–1328
22. L438A-Fw	GG$_{(iii)}$CTCGAGCGTTGCAATCATAGCTCTAGG	1302–1328
23. T439A-Fw	GG$_{(iii)}$CTCGAGCGTTGCAATCATAACTGCAGGTCGTCATTTG	1302–1338
24. G440A-Fw	GG$_{(iii)}$CTCGAGCGTTGCAATCATAACTCTAGCTCGTCATTTG	1302–1338
25. R441A-Fw	GG$_{(iii)}$CTCGAGCGTTGCAATCATAACTCTAGGTGCTCATTTG	1302–1338
26. H442A-Rv	TTG$_{(iiii)}$GTTAACGTTATCGTGTTCAAAGCACGAC	1328–1355
27. L443A-Rv	TTG$_{(iiii)}$GTTAACGTTATCGTGTTCGCATGACG	1330–1355
28. N444AA-Rv	TTG$_{(iiii)}$GTTAACGTTATCGTGGCCAAATGACG	1330–1355
29. T445A-Rv	TTG$_{(iiii)}$GTTAACGTTATCGCGTTCAAATGACG	1330–1355
30. I446A-Rv	TTG$_{(iiii)}$GTTAACGTTGCCGTGTTCAAATGACG	1330–1355
31. T447A-Rv	TTG$_{(iiii)}$GTTAACGCTATCGTGTTCAAATGACG	1330–1355
32. L448A-Fw	ACGATAACGGCAACCAAAACATTC	1342–1365
33. L448A-Rv	GTTTTGGTTGCCGTTATCGTGTTC	1338–1361
34. T449A-Fw	ACGATAACGTTAGCCAAAACATTC	1342–1365
35. T449A-Rv	GTTTTGGTTAACGCTATCGTGTTC	1338–1361
36. VAI/AAA-Fw	GG$_{(iii)}$CTCGAGCGCTGCAGCCATAACTCTAG	1302–1327
37. ILT/AAA-Fw	GG$_{(iii)}$CTCGAGCGTTGCAATCGCAGCTGCAGGTCGTC	1302–1333
38. GRH/AAA-Fw	CTAGCTGCTGCTTTGAACACG	1324–1344
39. GRH/AAA-Rv	CAAAGCAGCAGCTAGAGTTATG	1317–1338
40. LNT/AAA-Fw	CATGCGGCCGCGATAACGTTAAC	1333–1355
41. LNT/AAA-Rv	TATCGCGGCCGCATGACGACC	1327–1347
42. ITLT/AAAA-Fw	ACGGCAGCGGCAGCCAAAACATTC	1342–1365
43. ITLT/AAAA-Rv	TTTGGCTGCCGCTGCCGTGTTCAA	1336–1359
44. VAI/SSS-Fw	TGG$_{(iii)}$CTCGAGCTCTTCATCCATAACTCTAGG	1302–1328
45. VAI/RRR-Fw	TGG$_{(iii)}$CTCGAGCAGAAGAAGAATAACTCTAGG	1302–1328
46. V434R-Fw	TGG$_{(iii)}$CTCGAGCAGAGCAATCATAACTCTAGG	1302–1328
47. A435R-Fw	TGG$_{(iii)}$CTCGAGCGTTAGAATCATAACTCTAGG	1302–1328
48. I436R-Fw	TGG$_{(iii)}$CTCGAGCGTTGCAAGAATAACTCTAGG	1302–1328

*Position when the first letter of the initiation codon is 1. Restriction sites of *Bam*HI, *Sph*I, *Xho*I, and *Hin*cII are underlined (i), (ii), (iii), and (iiii), respectively. The positions of *Bam*HI, *Xho*I, and *Hin*cII site are 1034, 1302, and 1350, respectively. Fw and Rv indicate primers for forward and reverse primers in PCR, respectively.

mide gel electrophoresis on a 10% acrylamide gel, and the separated proteins were transferred to a membrane filter (GHVP, Millipore) (*40*). The membranes were treated with anti-GFP serum (Molecular Probe) or anti-Sec12p polyclonal antibodies (a kind gift from Dr. Akihiko Nakano, University of Tokyo). Immunoreactive bands were visualized by means of the enhanced chemiluminesence method, as described previously (Amersham Pharmacia) (*41*).

Other Procedures—All DNA manipulations were performed according to published procedures (*42*). Proteins were measured as described previously (*43*). DNA sequencing was performed by the dideoxy chain termination method (*44*) with an ABI 377 DNA sequencer.

Materials—Restriction enzymes, KOD DNA polymerase, and T4 DNA ligase were purchased from Toyobo and New England Biolabs. The oligonucleotides used in

Downloaded from http://jb.oxfordjournals.org/ at Changhua Christian Hospital on September 29, 2012

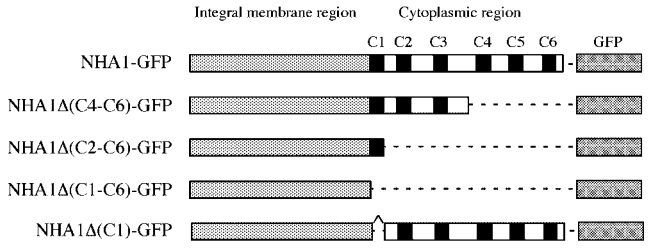

Fig. 1. **Schematic illustration of NHA1-GFP fusion proteins.** The transmembrane domain shown by the shadowed boxes comprises residues between 1 and 433. This putative integral membrane domain was previously predicted on hydropathy plot analysis. The conserved C1 to C6 domains in the hydrophilic tail domain (indicated by shadowing) comprise residues 434 to 449, 465 to 487, 526 to 540, 694 to 717, 787 to 815, and 919 to 944, respectively. The truncated forms of Nha1p include the following residues: NHA1Δ(C4-C6), 1–647; NHA1Δ(C2-C6), 1–449; NHA1Δ(C1-C6), 1–443; and NHA1Δ(C1), 1–433 and 450–985. GFP was fused to the C-terminus of each Nha1p derivative.

this study were synthesized by Invitrogen. Other materials were of the highest grade commercially available.

RESULTS

Effects of Deletions of the Cytoplasmic Domains of the Na^+/H^+ Antiporter 1 (Nha1p) on Salinity-Sensitivity—We previously showed that over-expression of carboxy-teminal truncations of Nha1p affects the growth of cells under conditions of high salinity (*27*). In those experiments the truncated forms were overproduced under the control of the efficient *GAP* promoter of the high-copy expression vector pKT10 (*35*). Here we expressed Nha1p truncations from the *NHA1* promoter to provide a lower level of protein and to reduce any consequences of over-expression. In order to localize Nha1p expression *in vivo*, we created C-terminal fusions of each Nha1p construct with the green fluorescence protein (GFP) (Fig. 1). Cells transformed with the full-length *NHA1-GFP* fusion construct were resistant to high salinity, as found for wild type cells (Fig. 2) and for *nha1Δ::LEU2* mutant SK5 transformed with *NHA1* alone (data not shown), implying that the GFP fusion protein is a functional Na^+/H^+ antiporter and that it acts to reduce the intracellular Na^+ concentration as efficiently as the wild type Nha1p. The concentration range of NaCl found to inhibit the growth of SK5 was 0.4 to 0.6 M, while at these concentrations SK5 transformed with the wild type *NHA1-GFP* fusion grew at a rate of 85–80% of that of control cells in medium without NaCl. Truncation of Nha1p by removal of the C4 to C6 domains permitted growth at concentrations of greater than 0.6 M (Fig. 2 B). In sharp contrast, loss of the C2 to C6 domains strongly inhibited growth under high salinity conditions. Further truncation resulting in loss of the C1 domain led to even more severe growth retardation than for the C2-C6 truncation (Fig. 2B). Internal deletion of the C1 domain also caused similar retardation of growth (data not shown). These results, except for that concerning the C1 internal deletion, are essentially the same as those obtained for Nha1p truncations expressed under the strong *GAP* promoter of pKT10. These results suggest

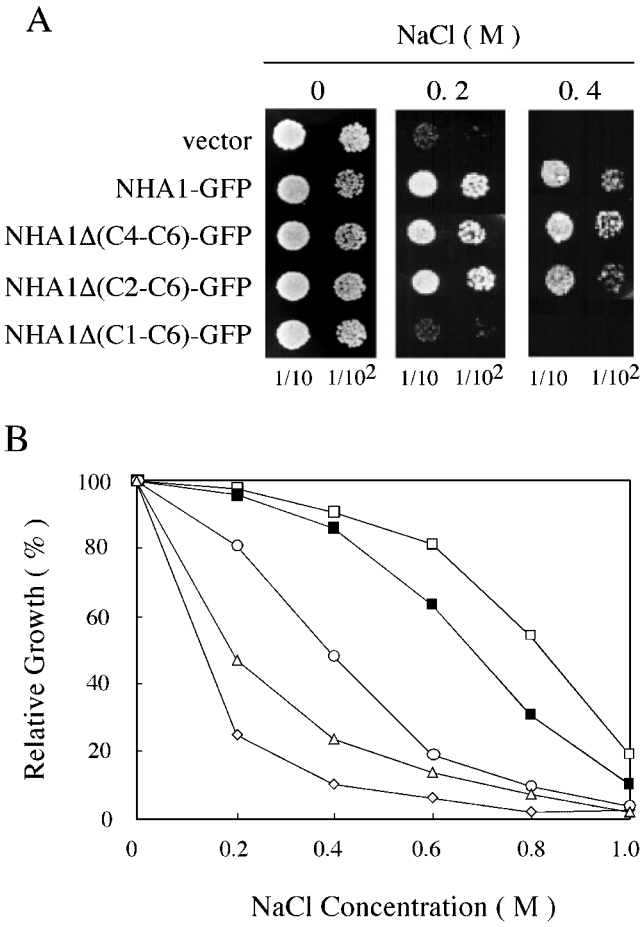

Fig. 2. **The growth of cells transformed with Nha1p truncation derivatives is inhibited under conditions of high salinity.** (A) SK5 (*nha1*Δ, *ena1-4*Δ) cells transformed with the Nha1p truncation forms shown in Fig. 1 were diluted serially and then spotted onto SD plates, pH 5.5 supplemented with NaCl as indicated. The plates were incubated at 30°C for 4 days. (B) SK5 transformants with the vector alone (diamonds), wild-type NHA1-GFP (solid squares), NHA1Δ (C4-C6)-GFP (open squares), NHA1D(C2-C6)-GFP (circies), or NHA1Δ(C1-C6)-GFP (triangles) were inoculated into 5 ml SD medium supplemented with the indicated concentrations of NaCl and then cultured at 30°C with vigorous shaking. The growth rate was spectrophotometrically determined (600 nm) after 24 h incubation at 30°C. The relative growth rate was calculated as described under "MATERIALS AND METHODS" and is presented as the percentage of the growth rate of cells cultured in medium without NaCl.

that the C1 and C2-C3 domains promote, and the C4-C6 domain inhibits growth under conditions of high salinity through influences on antiporter activity, as proposed previously (*27*). The phenotype of cells expressing Nha1p with the deletion of the C1 domain strongly supports the idea that this domain plays an essential role in antiporter activity.

Cellular Localization of Nha1p-GFP Fusions—Nha1p-GFP fusions were localized in transformed cells by fluorescence microscopy. While fluorescence due to GFP alone was found throughout the cell (Fig. 3A), strong signals were observed on the membrane surface of cells expressing the Nha1pΔ(C4-C6)-GFP and Nha1pΔ(C2-C6)-GFP fusions as well as the wild type Nha1p-GFP

Downloaded from http://jb.oxfordjournals.org/ at Changhua Christian Hospital on September 29, 2012

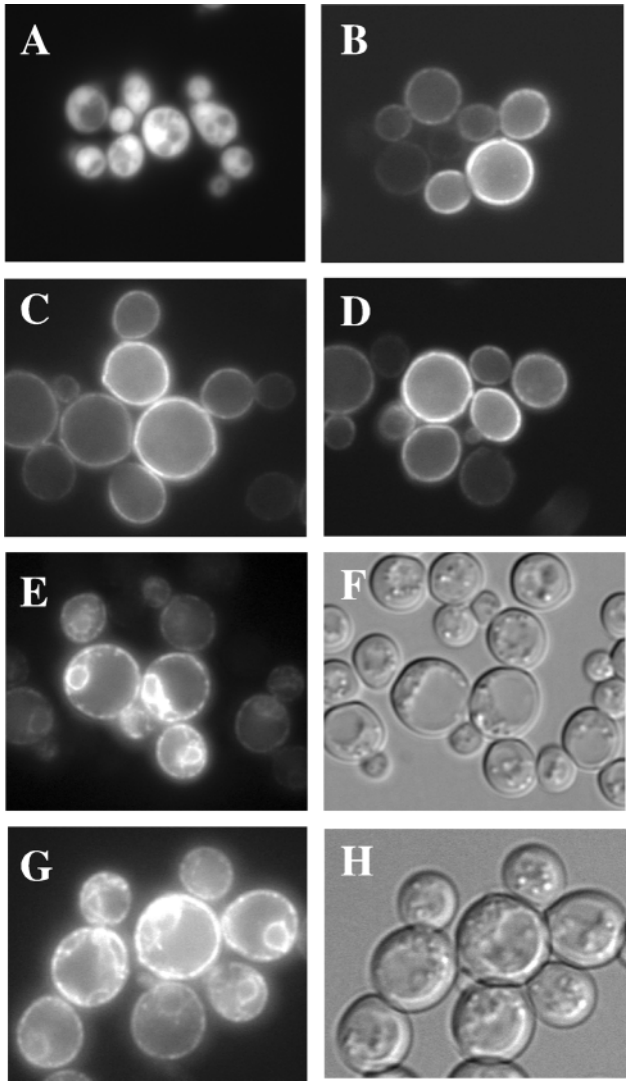

Fig. 3. **Cellular localization of Nha1p-GFP fusions.** SK5 (*nha1*Δ, *ena1-4*Δ) cells transformed with GFP alone (A), wild type NHA1-GFP (B), NHA1Δ(C4-C6)-GFP (C), NHA1Δ(C2-C6)-GFP (D), NHA1Δ(C1-C6)-GFP (E, F), or NHA1ΔC1-GFP (G, H) were grown at 30°C to the logarithmic phase, and then observed by fluorescence microscopy. Fluorescence microscopic images (E, G) and Nomarski microscopic images (F, H) of cells transformed with NHA1Δ(C1-C6)-GFP and NHA1ΔC1-GFP are shown.

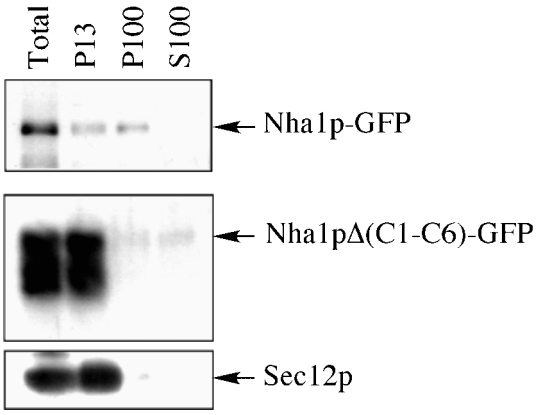

Fig. 4. **Intracellular distribution of Nha1p-GFP fusions.** Proteins prepared from cells expressing the full-length Nha1p-GFP or Nha1pΔ(C1-C6)-GFP were prepared as described under "MATERIALS AND METHODS," and then subjected to Western blot analysis with antibodies against GFP and Sec12p.

fusion (Fig. 3, B, C, and D). These results suggest that most of the C-terminal tail, up to the C2 domain, is not required for the targeting of Nha1p to the cytoplasmic membrane. However, removal of the entire C-terminus, including the C1 domain, caused most of the truncated Nha1p-GFP fusions to appear in an intracellular compartment peripheral to the nucleus (Fig. 3E). This compartment was identified as the ER on comparison of the pattern of fluorescence with images obtained on Nomarski microscopy (Fig. 3, E and F). The internal deletion of the C1 domain from the full-length Nha1p also caused Nha1p to be localized to the ER (Fig. 3, G and H). These results clearly show that the C1 region, but not the rest of the C-terminal tail, plays a crucial role in directing Nha1p to the cytoplasmic membrane. These results also support the idea that changes in the salt sensitivity of cells expressing truncated forms Nha1pΔ(C4-C6)-GFP and Nha1pΔ(C2-C6)-GFP are due to changes in antiporter activity rather than to an alteration in Nha1p localization. In contrast, the decreased growth of transformants expressing Nha1pΔ(C1-C6) was revealed to be due to inappropriate localization of the truncated Nha1p-GFP to the ER rather than to a decrease in Nha1p activity.

Localization of the Nha1pΔ(C1-C6)-GFP fusion was also determined by fractionation of whole cellular proteins (Fig. 4). The wild type Nha1p-GFP fusion was found in the P100 fraction, which includes small endocytic vesicles and cytoplasmic membrane fragments, as well as in the P13 fraction, which includes the ER, Golgi apparatus and large cytoplasmic membrane fragments. However, Nha1pΔ(C1-C6)-GFP was found primarily in the P13 fraction. As a control, the marker Sec12p, which is known to be localized to the ER, was found mainly in the P13 fraction, as expected (*45*). These biochemical results also confirm that fluorescence signals are due to the Nha1p-GFP fusion but not to GFP alone. Overall, these results are consistent with the observations made on fluorescence microscopy.

C1 Domain Residues Required for the Localization of Nha1p to the Cytoplasmic Membrane—We next addressed how the C1 domain of Nha1p functions in localization. For this purpose, we constructed a series of deletion mutants containing a part of the C1 domain and determined their intracellular locations, as shown in Fig. 5A. An Nha1p truncation derivative containing residues 1–438 exhibited the same pattern of distribution as full-length Nha1p (Fig. 5B), demonstrating that the residues between Leu-439 and Thr-449 do not affect the influence of the C1 domain as to the localization of Nha1p. However, Nha1p derivatives containing residues 1–434 and 1–435 were found in the ER, like Nha1pΔC1-C6 (Fig. 3A, Nha1p with residues 1–433). These results demonstrate that residues Val-434, Ala-435, and Ile-436 are required for the targeting of Nha1p to the cytoplasmic membrane, and that a critical border is defined by residues Ileu-437 and Thr-438. Although Nha1pΔ(437–985)-GFP and Nha1pΔ(438–985)-GFP are mainly localized in the cyto-

Downloaded from http://jb.oxfordjournals.org/ at Changhua Christian Hospital on September 29, 2012

A

wild type	- - V H G S S V A I I T L G R H L N T I T L T K T F T - -
Δ(445-985)	- - V H G S S V A I I T L G R H L N
Δ(444-985)	- - V H G S S V A I I T L G R H L
Δ(443-985)	- - V H G S S V A I I T L G R H
Δ(442-985)	- - V H G S S V A I I T L G R
Δ(441-985)	- - V H G S S V A I I T L G
Δ(440-985)	- - V H G S S V A I I T L
Δ(439-985)	- - V H G S S V A I I T
Δ(438-985)	- - V H G S S V A I I
Δ(437-985)	- - V H G S S V A I
Δ(436-985)	- - V H G S S V A
Δ(435-985)	- - V H G S S V

B

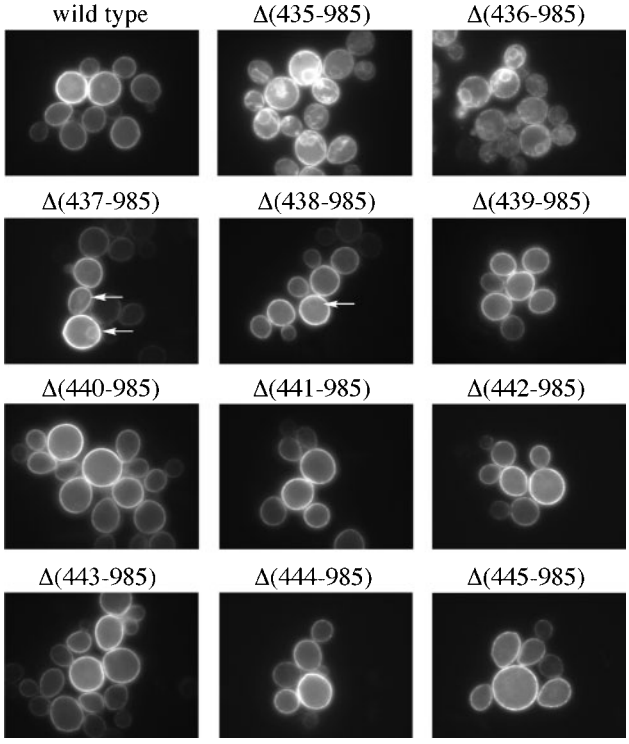

Fig. 5. **Localization of Nha1p derivatives with sequential deletions affecting the C1 domain.** (A) Amino acid sequences of mutant C1 domains. (B) SK5 cells expressing Nha1p C1 deletion derivatives were grown at 30°C to the logarithmic phase, and then Nha1p-GFP fusions were localized by fluorescence microscopy. SK5 cells expressing Nha1p-GFP with complete deletion of the C1 domain were grown at 30°C to the logarithmic phase, and then Nha1p-GFP fusions were localized by fluorescence microscopy. Arrows indicate a peripheral region, likely the ER, where fluorescence is observed.

plasmic membrane, a small but significant portion of these truncated proteins was also found in the peripheral region of the nucleus, possibly in the ER. Nonetheless, these truncation derivatives have a minimal structure sufficient for proper localization. We therefore conclude that C1 comprises two independent portions: one consisting of residues Val-434, Ala-435, and Ile-436 is essential

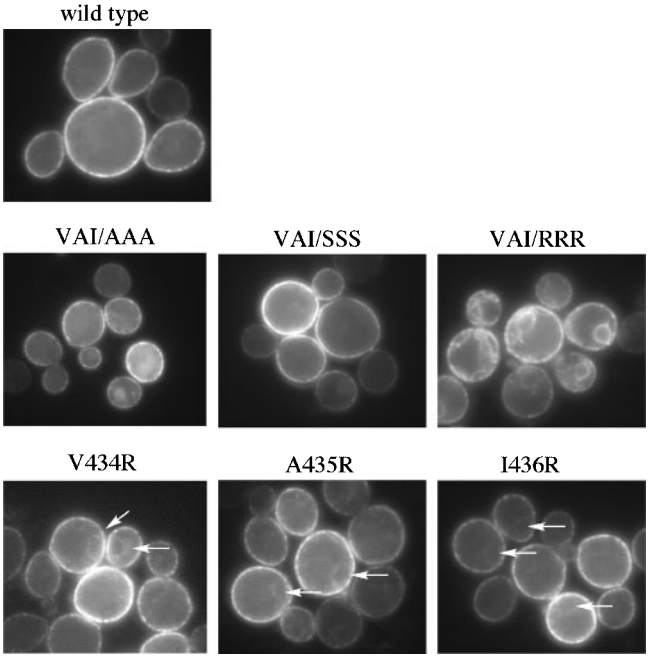

Fig. 6. **Effect of replacement of C1 residues by various amino acids on the localization of Nha1p to the cytoplasmic membrane.** Subcellular localization of Nha1p-GFP fusions with alanine, serine, or arginine substitutions. VAI/SSS and VAI/RRR indicate replacement of Val-434, Ala-435, and Ile-436 by three serines and arginines, respectively. Single amino-acid substitutions are denoted as V434R (replacement of Val-434 by arginine), A435R, and I436R. Cells expressing mutant Nha1p-GFP fusions were cultured as described in the legend to Fig. 2.

for localization, and the other consisting of residues 439 to 449 is not required for localization.

We next replaced each C1 residue by alanine and determined the localization of the resulting mutant Nha1p-GFP derivatives. As expected, alanine mutations affecting residues 439 through 449 had no effect on the localization (data not shown), consistent with the observations made with truncated Nha1p derivatives. Replacement of Val-434, Ala-435, and Il-436 by Ala also did not cause a shift in Nha1p localization (data not shown). Then a series of other derivatives was constructed for these three residues. Surprisingly, replacement by three alanines or serines did not affect the localization (Fig. 6), suggesting that the hydrophobicity of the three residues is not the key factor. These results also excluded the possibility of that the three residues play a role as a specific sequence motif. On the other hand, replacement by three arginines did cause a clear shift of Nha1p-GFP to the ER area like Nha1pΔC1 (Fig. 6). Replacement of each of the three residues by Arg (Val-434-Arg, Ala-435-Arg, and Ile-436-Arg) affected the localization slightly (Fig. 6). These results implied that the structure comprising Val-434, Ala-435, and Ile-436, especially the total volume occupied by the three residues, may play a crucial role in the proper localization of Nha1p to the cytoplasmic membrane.

Effects of Sec Mutations on the Localization of Nha1— Since we found the accumulation of Nha1p-GFP at an ER-like structure with the mutations in C1, we examined

Downloaded from http://jb.oxfordjournals.org/ at Changhua Christian Hospital on September 29, 2012

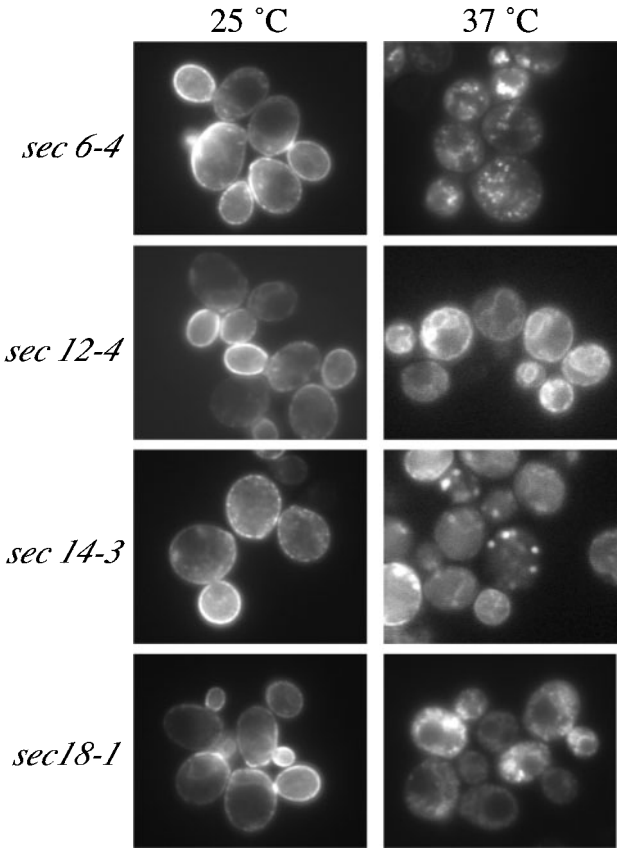

Fig. 7. **Effects of sec mutations on localization of NHA1-GFP fusions.** *sec6-4, sec12-4, sec14-3,* or *sec18-1* cells transformed with the NHA1-GFP fusion were grown at 25°C to the logarithmic phase, transferred to 37°C for 2 h or maintained at 25°C, fixed, and then examined by fluorescence microscopy to determine the intracellular locations of the Nha1p-GFP fusion proteins.

whether or not Nha1p is localized to the cytoplasmic membrane through the known secretory pathway. *SEC6*, *SEC12*, *SEC14*, and *SEC18* have been shown to be essential for the cytoplasmic trafficking of membrane vesicles and secretory proteins in *S. cerevisiae* (*30*). Here we examined whether or not temperature-sensitive mutations of these genes affect the localization of Nha1p. As shown in Fig. 7A, at a non-permissive temperature (37°C) for all of these *sec* mutations, the Nha1p-GFP fusion was not localized to the cytoplasmic membrane as in wild type cells. The *sec6-4* mutation is known to inhibit the fusion of secretory vesicles to the cytoplasmic membrane. In this mutant, Nha1p-GFP-specific fluorescence signals were observed to accumulate at 37°C and to form dot-like structures, possibly secretory vesicles. The *sec 12-4* mutation interferes with the release of COP II vesicles from the ER. With this mutant, Nha1p-GFP-specific fluorescence accumulated at the peripheral region of the nucleus, possibly in the ER, as expected. The patterns of accumulation of Nha1pΔC1-GFP and Nha1p-GFP with

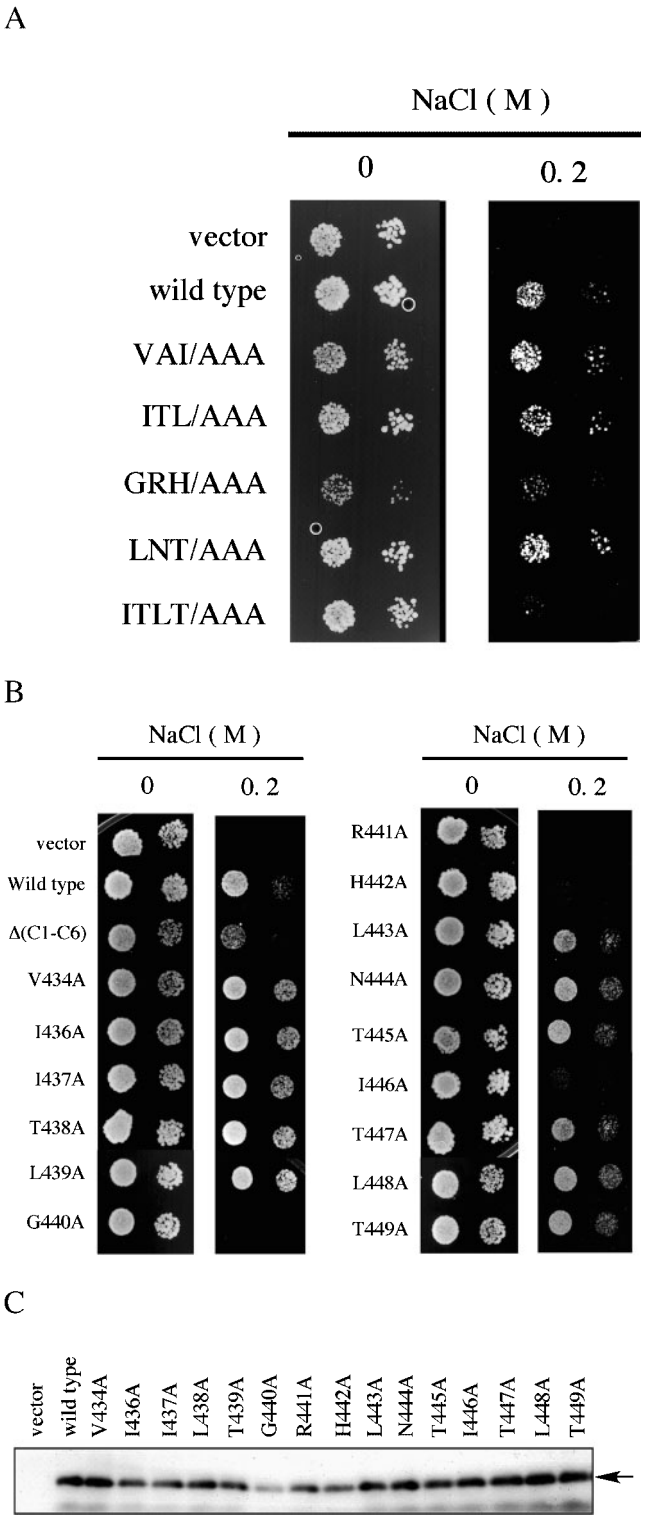

Fig. 8. **Effect of C1 single or multiple residue replacement by alanine on Nha1p activity.** (A) SK5 cells expressing Nha1p alanine triple substitution derivatives were diluted serially and the spotted onto SD plates, pH 5.5, supplemented with NaCl as indicated. The plates were incubated at 30°C for 4 days. The target sequences, VAI, ITL, GRH, LNT, and ITLT, correspond to those shown in the sequence of the wild type in Fig. 5A. (B) SK5 cells transformed with Nha1p alanine single substitution derivatives were cultured as described in Fig. 2, diluted serially, and then spotted onto SD plates, pH 5.5, supplemented with 0 or 0.2 M NaCl. The plates were incubated at 30°C for 4 days. (C) Whole cell extracts prepared from alanine substitution mutants were subjected to SDS polyacrylamide gel electrophoresis and Western blot analyses.

Downloaded from http://jb.oxfordjournals.org/ at Changhua Christian Hospital on September 29, 2012

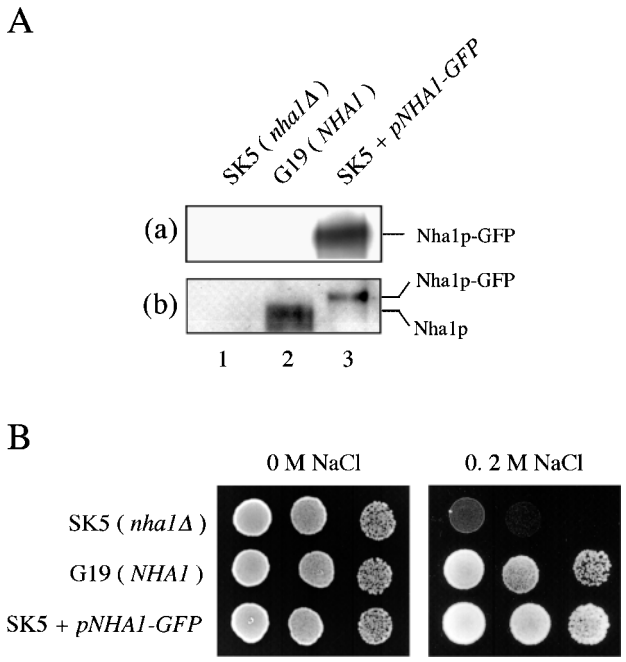

Fig. 9. **Expression of Nha1p and Nha1p-GFP, and salinity resistant cell-growth.** (A) Whole cell extracts prepared from SK5 (*nha1*Δ, *ena1-4*Δ), G19 (*NHA1*, *ena1-4*Δ), and SK5 with the expression plasmid of Nha1p-GFP were subjected to SDS polyacrylamide gel electrophoresis and Western blot analyses. (a) 15 μg protein in the total cell lysate was applied for lanes 1, 2, and 3. (b) 15 μg and 0.3 μg protein in the total cell lysate was applied to lanes 1 and 2, and lane 3, respectively. (B) Cells of SK5, G19, or SK5 expressing NHA1-GFP were diluted serially and then spotted onto SD plates, pH 5.5, supplemented with NaCl as indicated. The plates were incubated at 30°C for 4 days.

VAI/RRR substitutions are similar to this, supporting ER-accumulation of Nha1pΔC1-GFP and Nha1p-GFP with VAI/RRR substitutions. The *sec14-3* mutation has been shown to inhibit the formation of secretory vesicles in the Golgi apparatus. With this background, fluorescence signals accumulated in the cytoplasm as dot-like structures. Finally, *SEC18* is known to be essential for the fusion process, and the *sec18-1* mutation also causes trafficked vesicles to accumulate in the cytoplasm. In *sec18-1* cells, these vesicles exhibited Nha1p-GFP-specific fluorescence. These results constitute evidence that the cytoplasmic trafficking of Nha1p is dependent on previously identified *sec* gene functions and that Nha1p is routed through the proposed secretory pathway (*30*).

C1 Residues Important for Growth in the Presence of Salinity—To assess the functional roles of C1 domain residues in antiporter activity during growth in high-salt medium, a series of Nha1p alanine scanning mutants was created. Replacement of residues Gly-Arg-His (440–442) or Ile-Thr-Leu-Thr (446–449) with three or four alanine residues, respectively, caused a dramatic decrease in the growth of cells under conditions of high salinity (Fig. 8A). In contrast, other triple alanine replacements in the C1 domain had no effect. Thus, specific regions in the second portion of the C1 domain are required for resistance to salinity. Substitution of single residues with alanine revealed that the G440A, R441A, H442A, and I446A single mutations inhibited growth under conditions of high salinity (Fig. 8B), consistent with the results obtained for triple-residue replacement. These mutant Nha1ps are localized to the cytoplasmic membrane, like the wild type Nha1p. Therefore, these residues may play a key role in antiporter activity but not localization. The overall level of the Nha1p G440A mutant was reduced in total cell lysates (Fig. 8C), and the levels of the R441A and H442A mutant proteins were also slightly decreased (Fig. 8C). While we conclude that the I446A mutation inhibits growth under high salt conditions by possibly decreasing antiporter activity, the reduced rate of growth of the G440A mutant might be due both to a decrease in antiporter activity and a reduction in the level of protein. In this connection, it should be noted that the expressed Nha1p level in G19 cells is approximately fifty times lower than that of exogenously expressed Nha1p-GFP (Fig. 9A). Although the expression level of Nha1p is much lower in G19 than SK5 cells with Nha1p-GFP, the high salinity-resistant cell-growth of G19 is equivalent to cell-growth level of SK5 with Nah1p-GFP. Therefore, the levels of the G440A as well as the R441A and H442A mutant Nha1p expressed from the same vector as SK5 with Nha1p-GFP should be higher than Nha1p level in G19. These results suggest that decreased salinity resistant growth levels for the G440A, and R441A and H442A mutants are due to the altered antiporter activity rather than the expressed Nha1p levels. It is noteworthy that Nha1p (G440A)-GFP is localized only to the cytoplasmic membrane, *i.e.* not elsewhere, as found for Nha1pΔ(C1-C6). A portion of the mutant Nha1p may also undergo degradation.

DISCUSSION

Most eukaryotic Na^+/H^+ antiporters, including those of yeast, share a similar secondary structure (*8*, *27*). The two-domain structure comprises a hydrophobic integral membrane region and a hydrophilic cytoplasmic tail region. Extensive studies on mammalian NHEs have been undertaken to find regulators of antiport activity and proteins that interact with the cytoplasmic tail region (*13–20*). It has been proposed that calmodulin binds to the middle of the C-terminal tail of NHE1 and triggers antiporter activity by releasing the inhibition imposed by the C-terminal tail (*13*). However, the molecular mechanism by which calmodulin influences the Na^+/H^+ antiport with respect to the tail domain and interacting proteins has not been studied in detail, especially in the context of the two-domain structure. To address this issue, we have used the yeast Nha1p as a model to determine the functional significance of the two-domain structure at the amino acid level. We have carried out detailed structure-function relationship analysis of small domains in the hydrophilic tail of Nha1p proximal to the integral membrane region, these domains being conserved among yeast species.

The C1 domain, consisting of sixteen residues, was confirmed to be important for Nha1p function. Here we present evidence that C1 is further divisible into two functionally different portions. The first, consisting of three residues (Val-434, Ala-435, and Ile-436), was found to play a crucial role in the targeting of Nha1p to the cytoplasmic membrane from the ER. Replacement of

Downloaded from http://jb.oxfordjournals.org/ at Changhua Christian Hospital on September 29, 2012

these residues by Arg but not by Ser or Ala caused a shift in the intracellular localization of Nha1p-GFP to the ER. Therefore the space volume occupied by these three residues rather than their electrostatic charges or hydrophobicity seems to play a specific role in the localization of Nha1p. Nha1pΔC1 might lose the proper conformation required for movement from the ER to the cytoplasmic membrane. In other words, the addition of the three residues to the integral membrane domain probably induces the formation of the normal conformation of Nha1p required for the proper localization. To our knowledge, this is the first finding of a structure in the hydrophilic tail region required for the intracellular targeting of the integral membrane domains of Na^+/H^+ antiporters that have a two-domain structure, including mammalian NHEs. Here, we showed that Nha1p is localized to the cytoplasmic membrane via the secretory pathway. The accumulation of Nha1pΔC1-GFP is similar to that of the *sec12-4* mutant at the non-permissive temperature, supporting the notion that Nha1ΔC1-GFP has a defect in the release of Nha1p from the ER. It remains to be determined in the future how the supposed normal conformation provided by C1 is involved in this step.

The second portion of the C1 domain, from Leu-439 to Thr-449, is not involved in the localization of Nha1p. Replacement of Gly-440, Arg-441, His-442, and Ile-446 by alanine revealed that these residues play a key role in the conferring of salinity-resistance. We previously showed that the growth of yeast cells is highly dependent on the Na^+ concentration in the culture medium (*27*). Furthermore, the intracellular concentration of Na^+ is higher in Nha1p-deficient mutants than in wild type cells (*27*). These results indicate that the growth rate as a function of the salt concentration may reflect the Na^+/H^+ antiporter activity, which suggests that this activity is influenced by Gly-440, Arg-441, His-442, and Ile-446. The *Schizosaccharomyces pombe* Na^+/H^+ antiporter Sod2p contains three Asp residues (Asp-241, Asp-266, and Asp-267, in putative integral membrane segments 7 and 8), which are reported to be important for antiporter activity (49). Therefore, the ion transport conduit is believed to reside in the integral membrane region. The second portion of the C1 domain might influence the ion transport pathway directly or indirectly. In this context, it is notable that the membrane peripheral regions of the inward rectifier K^+ channel (50) and the bacterial drug antiporter AcrB (51) are essential for the translocation of ions.

A detailed molecular mechanism for Na^+/H^+ antiporters, including mammalian NHEs, has not been elucidated thus far. Here we have demonstrated that domains distant from the putative ion transport channel in the integral membrane region are important for ion transport and also for intracellular localization. These findings may provide new clues relevant to the understanding of antiporter activities, not only that of yeast Nha1p but also that of mammalian NHEs.

This study was supported in part by Grants-in-Aid from the Ministry of Education, Science, Technology, Sports and Culture of Japan, the TERMO Science Foundation, and a program supported by CREST (Core Research for Evolutional Science and Technology of the Japan Science Technology Corporation).

REFERENCES

1. Padan, E. and Schuldiner, S. (1993) Na^+/H^+ antiporters, molecular devices that couple the Na^+ and H^+ circulation in cells. *J. Bioenerg. Biomembr.* **25**, 647–69
2. Padan, E. and Schuldiner, S. (1994) Molecular physiology of Na^+/H^+ antiporter, key transporters in circulation of Na^+ and H^+ in cells. *Biochim. Biophys. Acta* **1185**, 129–151
3. Counillon, L. and Pouyssegur, J. (2000) The expanding family of eukaryotic Na^+/H^+ exchangers. *J. Biol. Chem.* **275**, 1–4
4. Orlowski, J. and Grinstein, S. (1997) Na^+/H^+ exchangers of mammalian cells. *J. Biol. Chem.* **272**, 22373–22376
5. Blumwald, E. (2000) Sodium transport and salt tolerance in plants. *Curr. Opin. Cell Biol.* **12**, 431–434
6. Padan, E., Venturi, M., Gerchman, Y., and Dover, N. (2001) Na^+/H^+ antiporters. *Biochim. Biophys. Acta* **1185**, 129–151
7. Jia, Z.P., McCullough, N., Martel, R., Hemmingsen, S., and Young, P.G. (1992) Gene amplification at a locus encoding a putative Na^+/H^+ antiporter confers sodium and lithium tolerance in fission yeast. *EMBO J.* **11**, 1631–1640
8. Orlowski, J., Kandasamy, R.A., and Shull, G.E. (1992) Molecular cloning of putative members of the Na/H exchanger gene family. cDNA cloning, deduced amino acid sequence, and mRNA tissue expression of the rat Na/H exchanger NHE-1 and two structurally related proteins. *J. Biol. Chem.* **267**, 9331–9339
9. Baird, N.R., Orlowski, J., Szabo, E.Z., Zaun, H.C., Schultheis, P.J., Menon, A.G., and Shull, G.E. (1999) Molecular colning, genomic organization, and functional expression of Na^+/H^+ exchanger isoform 5 (NHE5) from human brain. *J. Biol. Chem.* **274**, 4377–4382
10. Numata, M., Petrecca, K., Lake, N., and Orlowski, J. (1998) Identification of a mitochondrial Na^+/H^+ exchanger. *J. Biol. Chem.* **273**, 6951–6959
11. Numata, M. and Orlowski, J. (2001) Molecular cloning and characterization of a novel (Na^+, K^+)/H^+ exchanger localized to the trans-Golgi network. *J. Biol. Chem.* **276**, 17387–17394
12. Goyal, S., Vanden Heuvel, G., and Aronson, P.S. (2003) Renal expression of novel Na^+/H^+ exchanger isoform NHE8. *Amer. J. Physiol. Renal Physiol.* **284**, F467–473
13. Bertrand, B., Wakabayashi, S., Ikeda, T., Pouyssegur, J., Shigekawa, M. (1994) The Na^+/H^+ exchanger isoform 1 (NHE1) is an novel member of the calmodulin-binding proteins. Identification and characterization of calmodulin-binding sites. *J. Biol. Chem.* **269**, 13703–13709
14. Lin, X. and Barber, D.L. (1996) A calcineurin homologous protein inhibits GTPase-stimulated Na-H exchange. *Proc. Natl Acad. Sci. USA* **93**, 12631–12636
15. Matsumoto, M., Miyake, Y., Nagita, M., Inoue, H., Shitakubo, D., Takemoto, K., Ohtsuka, C., Murakami, H., Nakamura, N., and Kanazawa, H. (2001) A serine/threonine kinase which causes apoptosis-like cell death interacts with a calcineurin B-like protein capable of binding Na^+/H^+ exchanger. *J. Biochem.* **130**, 217–225
16. Weinman, E.J., Steplock, D., Wang, Y., and Shenolikar, S. (1995) Characterization of a protein cofactor that mediates protein kinase A regulation of the renal brush border membrane Na^+-H^+ exchanger. *J. Clin. Invest.* **95**, 2143–2149
17. Denker, S.P., Huang, D.C., Orlowski, J., Furthmayr, H., and Barber, D.L. (2000) Direct binding of the Na-H exchanger NHE1 to ERM proteins regulates the cortical cytoskelton and cell shape independently of H(+) translocation. *Mol. Cell* **6**, 1425–1436
18. Lehoux, S., Abe, J., Florian, J.A., and Berk, B.C. (2001) 14-3-3 Binding to Na^+/H^+ exchanger isoform-1 is associated with serum-dependent activation of Na^+/H^+ exchange. *J. Biol. Chem.* **276**, 15794–15800

Downloaded from http://jb.oxfordjournals.org/ at Changhua Christian Hospital on September 29, 2012

19. Mailander, J., Muller-Esterl, W., and Dedio, J. (2001) Human homolog of mouse tescalcin associates with Na^+/H^+ exchanger type-1. *FEBS Lett.* **507**, 331–335
20. Pang, T., Su, X., Wakabayashi, S., and Shigekawa, M. (2001) Calcineurin homologous protein as an essential cofactor for Na^+/H^+ exchangers. *J. Biol. Chem.* **276**, 17367–17372
21. Prior, C., Potier, S., Souciet, J.L., and Sychrova, H. (1996) Characterization of the NHA1 gene encoding a Na^+/H^+-antiporter of the yeast *Saccharomyces cerevisiae*. *FEBS Lett.* **387**, 89–93
22. Nass, R., Cunningham, K.W., and Rao, R. (1997) Intracellular sequestration of sodium by a novel Na^+/H^+ exchanger in yeast is enhanced by mutations in the plasma membrane H^+-ATPase. Insights into mechanisms of sodium tolerance. *J. Biol. Chem.* **272**, 26145–26152
23. Miyazaki, E., Sakaguchi, M., Wakabayashi, S., Shigekawa, M., and Mihara, K. (2001) NHE6 protein possesses a signal peptide destined for endoplasmic reticulum membrane and localizes in secretory organelles of the cell. *J. Biol. Chem.* **276**, 49221–49227
24. Brett, C.L., Wei, Y., Donowitz, M., Rao, R. (2002) Human Na^+/H^+ exchanger isoform 6 is found in recycling endosomes of cells, not in mitochondria. *Amer. J. Physiol.* **282**, C1031–C1041
25. Bañuelos, M.A., Sychrová, H., Bleykasten-Grosshans, C., Souciet, J.L. and Potier, S. (1998) The Nha1 antiporter of *Saccharomyces cerevisiae* mediates sodium and potassium efflux. *Microbiology* **144**, 2749–2758
26. Kinclova, O., Ramos, J., Portier, S., and Sychrova, H. (2001) Functional study of the *Saccharomyces cerevisiae* Nha1p C-terminus. *Molecular Microbiol.* **40**, 856–868
27. Kamauchi, S., Mitsui, K., Ujike, S., Haga, M., Nakamura, N., Inoue, H., Sakajo, S., Ueda, M., Tanaka, A., and Kanazawa, H. (2002) Structurally and functionally conserved domains in the diverse hydrophillic carboxy-terminal halves of various yeast and fungal Na^+/H^+ antiporters (Nha1p). *J. Biochem.* **131**, 821–831
28. Banuelos, M.A., Klein, R.D., Alexander-Bowman, S.J., and Rodriguez-Navarro, A. (1995) A potassium transporter of the yeast *Schwanniomyces occidentalis* homologous to the Kup system of *Escherichia coli* has a high concentrative capacity. *EMBO J.* **14**, 3021–3027
29. Sikorski, R.S. and Hieter, P. (1989) A system of shuttle vectors and yeast host strains designed for efficient manipulation of DNA in *Saccharomyces cerevisiae*. *Genetics* **122**, 19–27
30. Novic, P., Field, C., and Schekman, R. (1980) Identification of 23 complementation groups required for post-translational events in the yeast secretory pathway. *Cell* **21**, 205–215
31. Sherman, F. (1991) Guide to yeast genetics and molecular biology in *Methods Enzymol.* (Guthrie, C. and Fink, G.R., eds.) Vol. **194**, pp. 3–21, Academic Press, New York
32. Messing, J. and Vieira, J. (1982) A new pair of M13 vectors for selecting either DNA strand of double-digest restriction fragments. *Gene* **19**, 269–276
33. Kanazawa, H., Miki, T., Tamura, F., Yura, T., and Futai, M. (1979) Specialized transducing phage lambda carrying the genes for coupling factor of oxidative phosphorylation of *Escherichia coli*: increased synthesis of coupling factor on induction of prophage lambda asn. *Proc. Natl Acad. Sci. USA* **76**, 1126–1130
34. Miki, J., Fujiwara, K., Tsuda, M., Tsuchiya, T., and, Kanazawa, H. (1990) Suppression mutations in the defective β subunit of F_1-ATPase from *Escherichia coli*. *J. Biol. Chem.* **265**, 21567–21572
35. Tanaka, K., Nakafuku, M., Tamanoi, F., Kaziro, Y., Matsumoto, K., and Toh-e, A. (1990) IRA2, a second gene of *Saccharomyces cerevisiae* that encodes a protein with a domain homologous to mammalian ras GTPase-activating protein. *Mol. Cell. Biol.* **10**, 4303–4313
36. Kohrer, K. and Emr, S. (1993) The yeast VPS17 gene encodes a membrane-associated protein required for the sorting of soluble vacuolar hydrolases. *J. Biol. Chem.* **268**, 559–569
37. Miki, J., Kusuki, H., Tsugumi, S., and Kanazawa, H. (1994) Amino acid replacements at binding sites of monoclonal antibody in the F_1-ATPase β subunit from *Escherichia coli* caused altered subunit interactions. *J. Biol. Chem.* **269**, 4227–4232
38. Gillespie, P.G. and Hudspeth, A.J. (1991) Chemiluminescence detection of proteins from single cells. *Proc. Natl Acad. Sci. USA* **88**, 2563–2567
39. Manitias, T., Fritsch, E.F., and Sambrook, J. (1982) *Molecular Cloning: A Laboratory Manual*, Cold Spring Harbor Laboratory, Cold Spring Harbor, New York
40. Lowly, O.H., Roseburrough, B.P., Farr, A.C. and Randall, R.J. (1951) Protein measurment with the folin phenol reagent. *J. Biol. Chem.* **197**, 265–275
41. Sanger, F., Coulson, A.R., Barrell, B.G., Smith, A.J.H., and Roe, B.A. (1980) Cloning in single-stranded bacteriophage as an aid to rapid DNA sequencing. *J. Mol. Biol.* **143**, 161–178
42. Novic, P., Ferro, S., and Schekman, R. (1981) Order of events in the yeast secretory pathway. *Cell* **25**, 461–469
43. Dibrov, P., Young, P.G., and Fliegel, L. (1998) Functional analysis of amino acid residues essential for activity in the Na^+/H^+ exchanger of fission yeast. *Biochemistry* **37**, 8282–8286
44. Nishida, M. and MacKinnon, R. (2002) Structural basis of inward rectification: cytoplasmic pore of the G protein-gated inward recifier GIRK1 at 1.8 Å resolution. *Cell* **111**, 957–965
45. Murakami, S., Nakashima, R., Yamashita, E., and Yamaguchi, A. (2002) Crystal structure of bacterial multidrug efflux transporter AcrB. *Nature* **419**, 587–593

Downloaded from http://jb.oxfordjournals.org/ at Changhua Christian Hospital on September 29, 2012